Seismic Cycles and Trend Predictions of Earthquakes in Sumatra–Andaman and Burmese Subduction Zones using Temporal b-value and Hurst Analysis

Article *in* Journal of the Geological Society of India · December 2018

DOI: 10.1007/s12594-018-1084-6

CITATIONS
4

READS
161

3 authors, including:

Diptansu Sengupta
Geological Survey of India
7 PUBLICATIONS **10** CITATIONS
SEE PROFILE

Basab Mukhopadhyay
Geological Survey of India
81 PUBLICATIONS **552** CITATIONS
SEE PROFILE

JOURNAL GEOLOGICAL SOCIETY OF INDIA
Vol.92, December 2018, pp.661-670

Seismic Cycles and Trend Predictions of Earthquakes in Sumatra – Andaman and Burmese Subduction Zones using Temporal b-value and Hurst Analysis

Diptansu Sengupta[1], Basab Mukhopadhyay[1,*] and Om Prakash Mishra[2]

[1]Geological Survey of India, Central Headquarters, 29 J L Nehru Road, Kolkata -700 016, India.

[2]ESSO — Ministry of Earth Sciences (MoES), Lodi Road, New Delhi, India.

E-mail: *basabmukhopadhyay@gmail.com*; diptansu.sengupta@gmail.com*

ABSTRACT

The annual b-value fluctuation patterns in Burmese subduction zone and Andaman – Sumatra subduction zone are evaluated from earthquake data (January 1990 to June 2016; Mw ≥ 4.3) to identify seismic cycles with sequential dynamic phases as described in the 'elastic failure model' of Main et al. (1989). Two seismic cycles have been identified in Andaman – Sumatra subduction zone, one started in 1990 and ended on 2004 with occurrence of great Sumatra earthquake (Mw 9.0) and the other started in 2005 and continuing till date with the phase of crack coalescence and fluid diffusion (3A&B). Similarly, the subduction zone of Burma shows evidence of one incomplete seismic cycle within 1990-2016 and presently undergoing the crack coalescence and fluid diffusion (3A&B) phase. The analysis has prompted to subdivide the area into thirteen smaller seismic blocks (A to M) to analyse area specific seismic trend and vulnerability analysis employing Hurst Statistics. Hurst plots with the dynamic phases of 'elastic failure model' of earthquake generation is compared to assess the blocks with high seismic vulnerability. The analysis suggest that north Andaman zone (block G) and north Burma fold belt (block M) are seismically most vulnerable. Moreover, the seismic vulnerability of Tripura fold belt and Bangladesh plain (block K) is equally high.

INTRODUCTION

In nature, moderate to large earthquakes occur in cycles. The seismic cycle can be attributed to lithospheric volume, which gives earthquakes and repeatedly rupture a given part of a specific fault. The seismic cycle occurs in three phases: inter-seismic slip, co-seismic slip, and post-seismic slip phases (e.g. Klotz et al., 2001; Wang et al, 2012). The period of slow accumulation of elastic strain after the occurrence of a moderate / large earthquake coincides with the frictional locking of a fault between earthquakes (the inter-seismic phase), and finally the fault suddenly ruptures to generate the earthquake (the co-seismic phase). On the other hand, the seismic cycles within a tectonic zone can also comprehended by the temporal fluctuation model of seismic b-values known as 'elastic failure model' developed by Main et al. (1989) under varying stress and constant strain condition. The analysis ultimately leads to identification of sequential dynamic phases through which a seismic volume undergoes before a major earthquake, such as (1) an elastic stress build-up, (2) strain hardening, (3) strain softening, (4) dynamic failure, (5) to generate an earthquake event, followed by an aftershock sequence, as a part of the seismic cycle (Main et al. 1989). This model has been applied on sequential moment release data of macro-earthquakes (Mw ≥ 4.3) from January 1990 to June 2016 on the area (bounding latitude 0° – 30° and longitude 87° – 98°) comprising of two distinct tectonic/seismic domains, Burmese subduction zone and Andaman – Sumatra subduction zone in the present study.

The study area is subdivided into thirteen smaller seismic blocks (A to M) solely depending on the regional deformation characteristics to determine the vulnerable areas more precisely. Hurst statistics and plots are used to identify the temporal cluster of earthquakes in the dataset. Further, attempt is made to compare the Hurst plot patterns with the dynamic phases of 'elastic failure model' of earthquake generation by Main et al. (1989), and to identify seismically most vulnerable block(s) within the study area. Striking similarities in the patterns of Hurst plots across these thirteen blocks and predictable occurrence of large earthquakes in relationship with the Hurst plot pattern have helped to identify the seismic blocks with the ability to spawn future large earthquakes.

Earthquake Catalogue with Uniform Mw and Moment Release Data

The earthquake data has been collected for the period from January 1990 to June 2016 from ISC database for latitudes 0° - 30° N and longitudes 87° E - 98° E. It is found that ISC provides earthquake magnitudes in different scales like M_S, mb etc. For a meaningful seismic analysis, it becomes crucial to convert the different magnitude scales to a uniform scale, moment magnitude (Mw) in the present case. The magnitude relations developed by Scordilis (2006) are utilised to convert M_S, mb to a uniform moment magnitude (Mw) for all earthquakes in the catalogue. The conversion of M_S and mb to Mw is carried out by the following equations (Scordilis, 2006) for different range of magnitudes M_S and mb.

$$Mw = 0.67(\pm 0.005)\ M_S + 2.07(\pm 0.03), \text{ for } 3.0 \le M_S \le 6.1 \quad (1)$$

$$Mw = 0.99(\pm 0.02)\ M_S + 0.08(\pm 0.13), \text{ for } 6.2 \le M_S \le 8.2 \quad (2)$$

$$Mw = 0.85(\pm 0.04)\ mb + 1.03(\pm 0.23), \text{ for } 3.5 \le mb \le 6.2 \quad (3)$$

For magnitude completeness, the earthquake data of latitudes 0° - 30N and longitudes 87°E - 98°E is evaluated through a methodology based on the assumption of self-similarity (Wiemer and Wyss, 2000). The analysis indicates a magnitude completeness (Mc ≥ 4.3) for the period January 1990 to June 2016. Further, the seismic-moment M_0 (in dyne cm) for individual earthquake event (Mw ≥ 4.3) is then calculated using the equation, $\log M_0 = 1.5Mw + 10.05$ (eq. 4) (Hanks and Kanamori, 1979; McGuire, 2004). Hence, the earthquake catalogue contains both magnitude (Mw) and moment release data for earthquakes. Following the definition of aftershocks notwithstanding, many authors (Chan and Chandler, 2001; Amor'ese et al., 2010) suggest to use of de-clustered catalogues in the computation of b-values. For de-clustering, it is essential to remove the dependent events, mainly foreshocks and aftershocks to make the b value statistically unbiased

0016-7622/2018-92-6-661/$ 1.00 © GEOL. SOC. INDIA | DOI: 10.1007/s12594-018-1084-6

and robust. The dataset were declustered using the procedure presented in Kafka and Walcott (1998). Hence, the aftershocks have been removed from the dataset but the trigger shocks are kept in Sumatra region (after Dasgupta et al. 2005, 2007a, 2007b) to calculate the temporal b-value.

SEISMICITY MAP AND TECTONIC SCENARIO

The earthquake data with magnitude (Mw) ≥ 4.3 are shown in Fig.1 with suitable magnitude bins along with regional tectonics (Dasgupta et al. 2000; Curray 2005). The area has experienced severe seismicity with incidence of many moderate to large earthquakes of Mw > 6.0. Some recent earthquakes of importance are the great 2004 Sumatra earthquake (26.12.2004, Mw 9.0), Nias earthquake (28.03.2005, Mw 8.6) along the plate interface and prominent strike-slip seismicity within Indo-Australian plate (10.01.2012, Mw 7.2; 11.04.2012, Mw 8.6 and 11.04.2012, Mw 8.2).

Tectonically, the study area consists of Burmese and Andaman – Sumatra subduction zones that constitute a prominent destructive plate margin of 2100 km strike length in the NE Indian Ocean and land part of India and Burma. The zone serves as the tectonic link between the western Pacific arc system in the south and the Himalayas in the north (Fig.2).

The zone comprises of the following broad tectonic domains. In Burma, the subduction zone is clearly discernible in a land environment delimited by Eastern Boundary Thrust (EBT) with a frontal fold belt of Tripura and Bangladesh, and a seismically stable Shan plateau in the back. The oblique ocean-ocean subduction of Indian plate under SE Asian plate in Andaman – Sumatra subduction zone is manifested by a prominent trench zone of Andaman and Sumatra in the west. The tectonic elements from west to east in Andaman – Sumatra subduction

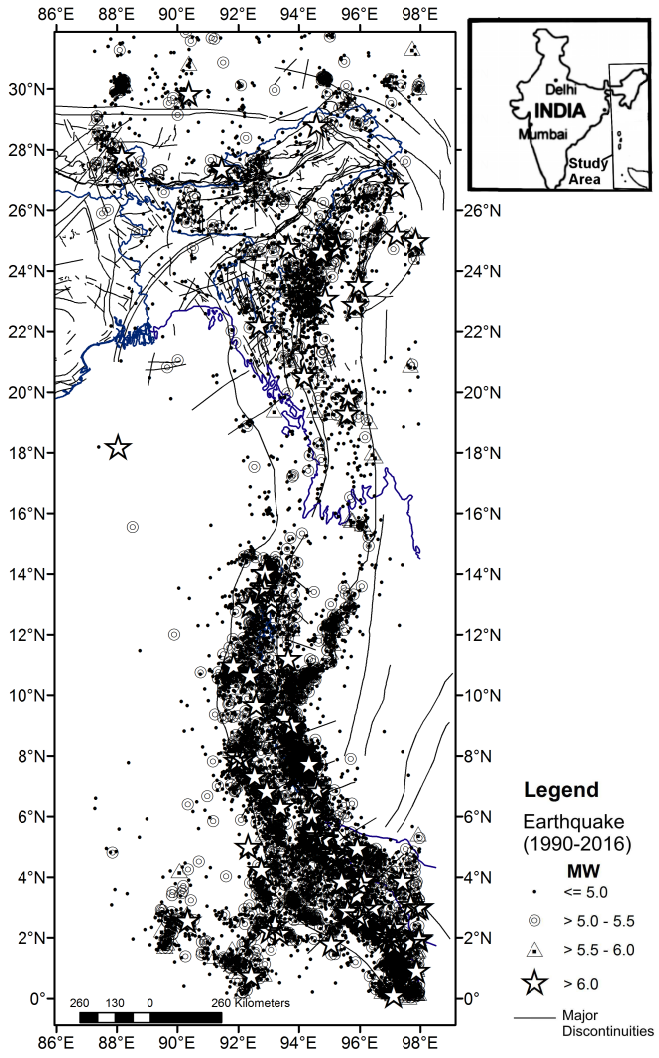

Fig.1. Epicentral map of Burmese subduction zone and Andaman – Sumatra subduction zone with earthquake data for the period: 1990–2016 in different magnitude bins. Inset shows the study area.

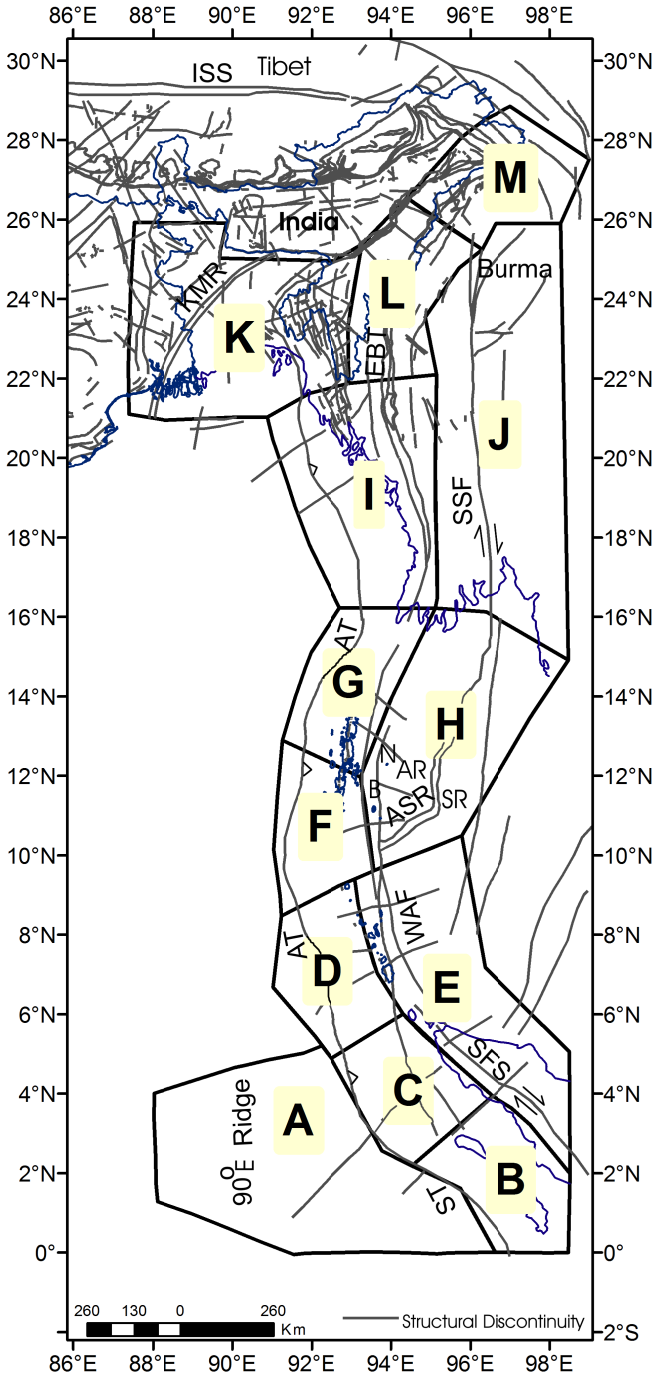

Fig.2. Spatial distribution of thirteen seismic blocks (A to M) delineated on the basis of variation of tectonic motif along the arc, seismogenesis, crustal heterogeneity and other geophysical parameters (see text) for Hurst analysis. The temporal b value analysis is done on Andaman – Sumatra Subduction zone (comprising of blocks B, C, D, F, G) and Burma subduction zone (blocks I, L and M) to understand seismic cycles within the dataset. AT – Andaman Trench, AR- Alcock Rise, ASR- Andaman Spreading Ridge, B – Barren Island Volcano, KMR – Kolkata Maimonsingh Ridge, ISS – Indus Psangpo Suture, SR – Sewell Rise, SSF – Shan Sagaing Fault, SFS – Sumatra Fault System, ST – Sumatra Trench, WAF – West Andaman Fault, N – Narcondam Island Volcano.

zone are a prominent trench (Andaman and Sumatra), an outer sedimentary ridge of Andaman–Nicobar–Nias Islands in between trench and the volcanic arc. The volcanic arc represents an active belt between Sumatra in the south and Burma in the north with several dormant volcanoes in the land part, active Barren Island, dormant Narcondam and several under-sea volcanoes in between. Further east, Andaman Spreading Ridge (ASR) underlying the Andaman Sea between Alcock Rise (AR) and Sewell Rise (SR) is related to the Neogene back arc spreading that occur through several short leaky transforms (Uyeda and Kanamori 1979). The southern extremity of the study area is an intense seismic coupled zone of offshore Sumatra, which is infamous to produce large earthquakes in the plate interface (Fig.2).

Earthquake focal mechanism studies (Dasgupta and Mukhopadhyay, 1993; Dasgupta et al. 2003; Mukhopadhyay et al. 2009b) further demonstrate that the upper lithosphere is under the influence of compressive stress, whereas, it is the extensional stress that operates in the top lithosphere below the back arc spreading centre in ASR. It is therefore logical to find difference in deformation pattern within different parts of the arc system as contrasting stress fields operate in the top lithosphere. The seismotectonic analysis has marked sixteen hinge faults across the trend of the arc with immobile western end and they have delimited the entire study area into several blocks of individual seismic characters (Dasgupta et al. 2003; Mukhopadhyay et al. 2009b).

METHODOLOGIES

The calculated b-value indicates tectonic parameter and represents properties of the seismic medium like stress and/or material conditions of the focal region (Kulhanek, 2005). The value of b varies 0.4-0.7 for intraplate, 0.7-1.0 for interplate and 1.0 -1.8 for oceanic regions. Whereas, Hurst statistics is generally used to identify the temporal clusters and significance of it in a time-series.

b-value Analysis

The *b*-value is calculated by the Maximum Likelihood Method (MLM, Aki, 1965) with the equation $b = (\mathrm{Log}_{10}\, e) / (M_{av} - M_{min})$ (eq. 5), where M_{av} is the mean magnitude above the threshold M_{min}. The maximum-likelihood method provides the least biased estimate of b-value (Aki 1965). Further, an estimate of the standard deviation (δb) of the error in *b*-value computation is obtained using $\delta b = 2.3b^2 \sqrt{\Sigma^{n}_{i=1} (M_i - M_{av})^2/n(n-1)}$ (eq. 6, Shi and Bolt, 1982), where n is the number of events of the given sample. As *b*-value is dependent on data, earthquake data is treated as per techniques described by Kulhanek (2005). The technique of b-value calculation as described in Kulhanek (2005) is useful to make the calculated b-value statistically robust and tectonically significant for further analysis.

Another popular method of estimation of b value by regression [Log N = a – bM (eq. 6), where N is the cumulative number of earthquakes per year of magnitude, 'a' is called the 'productivity'] is known as Least Squares Method (LSQ).

Generally, for *b* value estimation the MLM method is preferred over the least squares method (LSQ) in view of the uncertainties in the latter as demonstrated by Sandri and Marzocchi (2007).

Furthermore for the present study, the b-value is also calculated by LSQ method in some of the sectors by us to compare with the b value computed by MLM, they provide identical values.

Hurst Statistics

Hurst (1951, 1956) proposed a nonparametric statistical application popularly termed as Hurst statistics while working on long-term storage of reservoirs along river Nile in Egypt. He deduced a relationship that states $R/S \sim N^h$ where R is the maximum range of cumulative departure from mean annual discharge of river, N is the year of observations, S is the standard deviation of river discharge. Hurst approximated the coefficient h by another scalar K where K is equal to $\log(R/S)/\log_{10}(N/2)$. It is found that natural sequences with large number of observations follow Hurst phenomenon and yield a K value always greater than 0.5 (Wallis and Matalas, 1971). A Hurst exponent (K) close to 0.5 is indicative of a Brownian time series where there is no correlation between the present observations and an estimated result for future (Mandelbrot and Hudson, 2004). A Hurst exponent value between 0 and 0.5 is thus indicative of anti-persistent behaviour i.e. the tendency for the time series to revert to its long-term mean value. Whereas, a Hurst exponent (K) between 0.5 and 1.0 indicates persistent behaviour i.e. an increase in values will most likely to be followed by an increase in the short term, and a decrease in values will most likely to be followed by another decrease in the short term (Mansukhani, 2012) and hence indicating distinct clustering in datasets. Further, Hurst (1951, 1956) observed that a natural process (with large number of observations) occurring in irregular groups of high and low values show high K values greater than 0.5. Alternately, where the number of observations (n) is small, an estimator H is calculated by dividing the log-transformed ($\log_{10}$) observations into n number of subseries (Wallis and Matalas, 1970, 1971). For each sub-series the value of Rn/Sn is calculated. The slope of regression line in log(Rn/Sn)/log(n) plot gives the value of H. For large values of N, Chen and Hiscott (1999) and Mukhopadhyay et al. (2003, 2009a) observed that K value lies between 0.5 and 0.9.

The seismic moment values calculated by equation 4 of successive earthquake events for an individual zone are taken. To calculate K for N number of observations, the seismic moment values are transformed logarithmically ($\log_{10}$) base. Mean (M) and standard deviation (S) of the log transformed moment data are calculated. From each moment data, the mean is subtracted and then cumulative difference from the mean is computed by adding the values in the series. This cumulative departure from mean is plotted against year to generate the Hurst Plot. Range (R) is calculated as the difference between the maximum and the minimum value of the cumulative deviation in the Hurst plot, and K is calculated by the formula $\log (R/S) / \log_{10}(N/2)$, where N is the total number of observations.

The moment release pattern is graphically illustrated in Hurst plot where cumulative difference from the mean moment is plotted against sequential observation / year. The plot contains three distinct trends; positive, sub-horizontal and negative sloping segments. The significance of which is illustrated in the following section.

TEMPORAL b-value PRECURSORS AND SEISMIC CYCLES

The analysis of seismic cycle is most important to understand the present dynamics in a region to assess the seismic vulnerability. Accordingly, to determine the seismic cycles(s) two areas are delineated having contrasting tectonic motif and with the most concentration of earthquake data; (i) Benioff zone of Andaman – Sumatra sector [B to G (except block E) of Fig.2] (ii) The subduction zone of Burma (blocks I, L and M of Fig.2). Annual b-values and error in b-value calculation (see Table 1) for both zones by maximum likelihood method of Aki (1965) and by equation 6 (Shi and Bolt 1982) are calculted. The earthquakes with time – magnitude distribution, and b-values with error bars are shown against years for both the zones (Figs. 3 and 4) for further visualisation.

The temporal and spatial b-value in the Andaman – Sumatra sector reveal significant drop in b-value proceeding the time of occurrence of two large earthquakes (Ms ≥ 7) in 2002 and of the Mw 9.0 Sumatra Earthquake in 2004 (Nuannin, 2006; Nuannin et al., 2012). Dasgupta et al. (2007b) also report similar temporal variations of b where spatial distribution exhibits low b around the epicentres of the 2002 and 2004 events. The results of all these studies clearly brought out that the

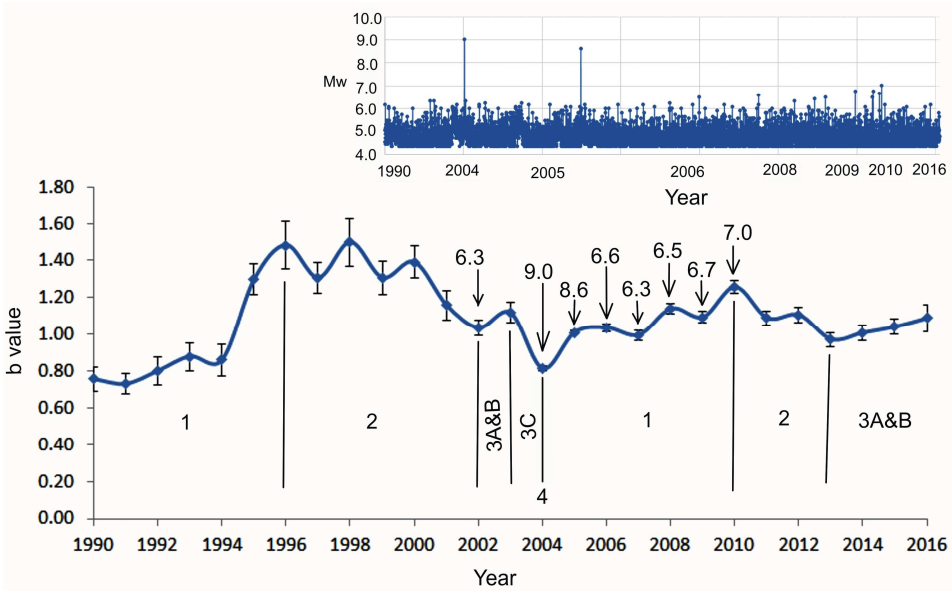

Fig.3. The earthquakes with time – magnitude distribution (upper panel), and temporal variation of seismic b-value with error bars (lower panel) in the Andaman – Sumatra subduction zone (comprising of blocks B, C, D, F and G of figure 2). The diagram shows a complete seismic cycle from 1990 to 2004 (ended with 2004 Sumatra earthquake (Mw 9.0)) and another incomplete seismic cycle from 2005 to till date. The diagram is divided into dynamic phases as per the 'elastic failure model' of Main et al. (1989): elastic stress build-up (1), strain hardening (2), strain softening (3), dynamic failure (4) to generate an earthquake event, followed by an aftershock sequence (5). In addition, 3A indicates crack coalescence, 3B fluid diffusion phase and 3C acceleration of fracture. Major shocks with magnitude are marked.

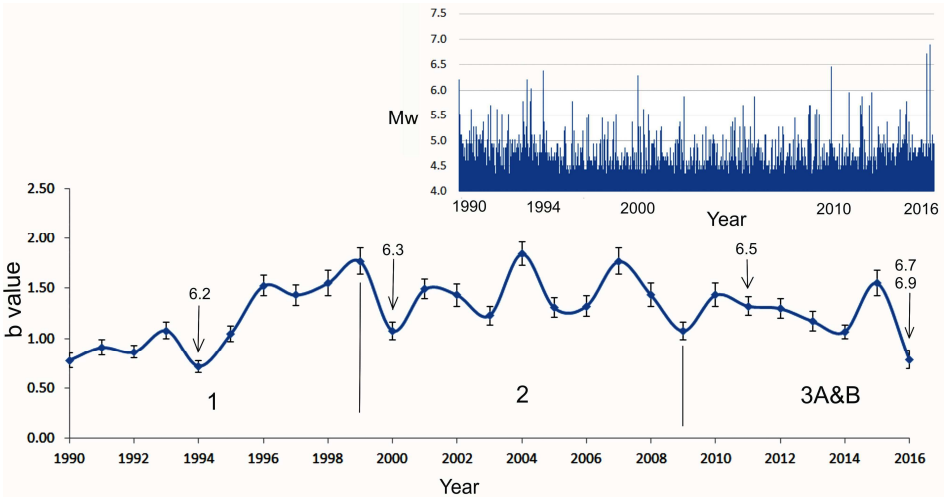

Fig.4. The earthquakes with time – magnitude distribution (upper panel), and temporal variation of seismic b-value with error bars (lower panel) in the Burma subduction zone (blocks I, L and M of figure 2). The diagram shows an incomplete seismic cycle from 1990 to till date. The diagram is divided into dynamic phases as per the 'elastic failure model' of Main et al. (1989): elastic stress build-up (1), strain hardening (2), strain softening (3), Crack coalescence phase (3A) and Fluid diffusion phase (3B). Major shocks with magnitude are marked.

low *b*-value and low fractal dimension are corresponding to locales for sizable magnitude earthquakes and further corroborated with locates of high stress regions (Srivastava et al. 2015). The annual b-value distribution of Andaman – Sumatra subduction zone (Fig.3) by the present study also shows significant low b value precursory trend prior to Mw 9.0 Sumatra event of 2004 but the value obtained is slightly higher than the value obtained by earlier studies mentioned above. The low b-values and high stress occur where the subducting and overriding plates are strongly coupled like the zone of Sumatra earthquake 2004 (see also Tormann et al. 2015 for similar analysis for 2011 Tohoku-oki earthquake of Japan). The analysis show the b-values are time dependent elastic failure model of earthquake generation as elaborated by Main et al. (1989). It shows a complete seismic cycle in between 1990 to 2004 (Fig.3) identified by this study which yields the great Sumatra earthquake (Mw 9.0) at the end. The cycle starts with an elastic stress build up (1) between 1990 and 1998, followed by strain hardening (2) between 1998 and 2002. Strain softening (3) started from 2002 and continued up to 2004, until the dynamic failure (4) occur in 2004 marked by great Sumatra earthquake (Mw 9.0) and its aftershock sequence (5) continued in 2005. The period of strain softening (3) is further separated into two distinct phases of crack coalescence and fluid diffusion (3A&B) from 2002 to 2003 and fracture acceleration (3C) from 2003 to 2004, based on the slope of the annual b-value curve after Main et al. (1989).

Another seismic cycle is envisaged in the zone that has started from 2005. The second cycle shows elastic stress build up (1) between 2005 and 2010 yielding several mega thrust earthquake sequences (Figure 3), followed by a strain hardening period (2) between 2010 and 2013. This is trailed by a strain-softening period started in 2013 and the same pattern probably continues to date. According to the

Table 1. Showing b-value (calculated by Maximum Likelihood Method of Aki, 1965) and error in b-value (calculated by equation of Shi and Bolt, 1982) of the Benioff zone of Andaman – Sumatra [blocks B to G (except E) of Fig.2] and the Benioff zone of Burma (blocks I, L and M of Fig.2).

	Benioff zone of Andaman – Sumatra				Benioff zone of Burma		
Year	No. of earth-quake data (Mw≥4.3)	b-value	Error in b-value	Year	No. of earth-quake data (Mw≥4.3)	b-value	Error in b-value
1990	33	0.76	0.07	1990	29	0.78	0.07
1991	41	0.73	0.06	1991	33	0.91	0.08
1992	28	0.80	0.08	1992	46	0.86	0.06
1993	33	0.88	0.08	1993	42	1.08	0.08
1994	25	0.86	0.09	1994	38	0.72	0.06
1995	58	1.30	0.09	1995	46	1.05	0.08
1996	32	1.48	0.13	1996	54	1.52	0.1
1997	60	1.31	0.08	1997	49	1.43	0.1
1998	35	1.50	0.13	1998	35	1.55	0.13
1999	56	1.31	0.09	1999	44	1.77	0.13
2000	64	1.39	0.09	2000	41	1.08	0.08
2001	54	1.16	0.08	2001	57	1.49	0.1
2002	165	1.04	0.04	2002	42	1.43	0.11
2003	98	1.12	0.06	2003	44	1.23	0.09
2004	871	0.81	0.01	2004	60	1.85	0.12
2005	2860	1.01	0.01	2005	45	1.31	0.1
2006	574	1.04	0.02	2006	45	1.32	0.1
2007	328	1.00	0.03	2007	45	1.77	0.13
2008	456	1.14	0.03	2008	37	1.43	0.12
2009	269	1.09	0.03	2009	39	1.08	0.09
2010	383	1.26	0.03	2010	36	1.43	0.12
2011	210	1.09	0.04	2011	51	1.32	0.09
2012	196	1.11	0.04	2012	48	1.30	0.09
2013	157	0.97	0.04	2013	38	1.17	0.1
2014	150	1.01	0.04	2014	62	1.07	0.07
2015	152	1.04	0.04	2015	39	1.55	0.12
2016	148	1.09	0.07	2016	58	0.78	0.09

diagram given by Main et al. (1989) the period of fracture acceleration defines by a sharp negative slope of the b-values. This phase is still absent in the annual b-value plot of Andaman-Sumatra Benioff zone. Therefore, it is concluded that the phase of crack coalescence and fluid diffusion (3A&B) is still going on in this area.

Similarly, Burma subduction zone (Fig.4) shows a single incomplete earthquake cycle as per Main et al. (1989) which starts with an elastic stress build up (1) in between 1990 and 1999, followed by a strain-hardening period (2) up to 2009. This follows by a strain-softening period (3) in between 2009 and 2016. Although the b-value of post 2015 period around Burma subduction zone takes a very sharp fall, it may coincide with the initiation of the fracture acceleration (3C) phase, which may follow by dynamic failure (4) in near future. Otherwise, this can still be well within the phase of crack coalescence and fluid diffusion (3A&B) phase (Main et al. 1989).

DELINEATION OF SEISMIC BLOCKS

Based on the study of seismic cycles discussed above it can be concluded that the regions approaching towards the dynamic failure but yet to record any major earthquake should be considered as the most vulnerable zones for future earthquake to occur. However, moderately large earthquake may also occur during the phases of crack coalescence and fluid diffusion (3A&B). Therefore, to study each smaller phases of a seismic cycle in greater details and to locate the earthquake prone areas more precisely, the entire study area has been subdivided into thirteen seismic blocks (A to M) based on their contrasting geo-tectonic characters (Fig.2). The geographical boundary of the blocks are delineated taking into consideration various factors, (i) variation in tectonic style, (ii) type of responsible faults for the earthquakes, (iii) ability to spawn large earthquake (Mw > 6) depending on present and past seismic records, (iv) presence of seismogenic transverse tear faults, (v) spatial clustering zones of moderate to large earthquakes, (vi) speed of shear waves in different sectors wherever available, (vii) contrasting stress fields operate in top lithosphere in different zones, (viii) differential crustal structure as deduced from tomographic studies and its bearing to regional / local tectonics, etc.

DISCUSSION

Temporal Clustering of Seismicity in the Blocks, Inferred from Hurst Plots

Hurst statistics has been applied on the seismic data of the blocks and Hurst K and corresponding b values are calculated and tabulated (Table 2). The relationship between Hurst K and b values in the blocks and its significance are discussed in details elsewhere by us (Mukhopadhyay and Sengupta, 2018). Moreover, Hurst plots (Figs. 5 - 12) corresponding to the ten seismic source blocks (B - G and I, K, L, M in Fig.2) for different seismic cycles have been analysed here. From the plots (Figs. 5 - 12), it can be inferred that the moment release in a block always occurs in alternate positive and negative sloping segments forming a wave like pattern. The positive segment is characterised by accelerated moment release within a short span of time, accompanied by clustering of larger magnitude earthquakes / seismic moments. The negative sloping segments define a temporal clustering of small magnitude earthquakes / seismic moments with possible high pore pressure perturbation. All plots attest moderate to high Hurst clustering coefficient (K) values. The Hurst statistics of blocks A to M shows moderate to high Hurst clustering coefficients values ranging in between 0.7 and 0.9 indicating stabilisation in the process of earthquake generation (Table 2). In the Sumatra-Andaman region, Tiwari and Krishnaveni (2015) have computed Hurst coefficient as 0.9 from earthquake recurrence time series and from other non-

Table 2. Characteristics of the Seismic Source Zones, A to Q of Fig. 2 with Hurst K and b values

Seismic Zone	Zone Name	Type of earth-quake source	Hurst K Value	b value with error
A	Indo-Australian Intraplate Zone	Strike slip (oblique slip)	0.7910	0.95±0.03
B	Nias Earthquake Zone	Thrust	0.7540	0.88±0.01
C	Sumatra Earthquake Zone	Thrust	0.7015	0.78±0.02
D	Nicober Island Zone	Thrust	0.7838	0.90±0.03
E	Sumatra Island Zone	Strike slip (oblique slip)	0.7952	0.83±0.02
F	South Andaman Zone	Thrust	0.7606	0.97±0.03
G	North Andaman Zone	Thrust	0.7702	0.99±0.03
H	Andaman Spreading Zone	Strike slip and Normal	0.8580	0.81±0.02
I	South Burma Zone	Strike slip and thrust	0.8552	0.91±0.05
J	Sagaing Fault Zone	Strike slip	0.7874	0.84±0.04
K	Tripura Fold Belt and Bangladesh Plain	Thrust and Strike slip (oblique slip)	0.7991	0.91±0.07
L	Central Burma Fold Thrust Belt	Strike slip (oblique slip) and Thrust	0.8415	0.93±0.06
M	North Burma Fold-Thrust Belt	Strike slip (oblique slip) and thrust	0.8606	0.85±0.05

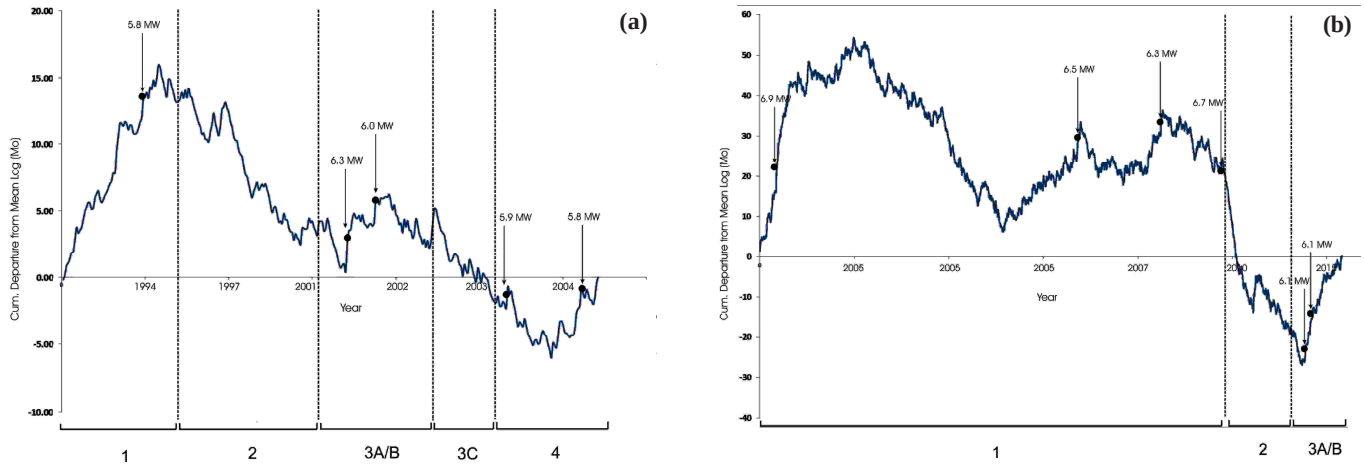

Fig.5. Hurst plot of years against cumulative difference from mean Log cumulative moment release data of earthquakes of Block B (Andaman – Sumatra subduction zone) **(a)** for the first earthquake cycle (1990-2004), ended with 2004 Sumatra earthquake (Mw 9.0). **(b)** for the second incomplete earthquake cycle (2005-2016). The phases are marked - elastic stress build-up (1), strain hardening (2), strain softening (3), dynamic failure (4) to generate earthquake event. Phase 3 is subdivided into 3A - crack coalescence, 3B - fluid diffusion phase and 3C- acceleration of fracture.

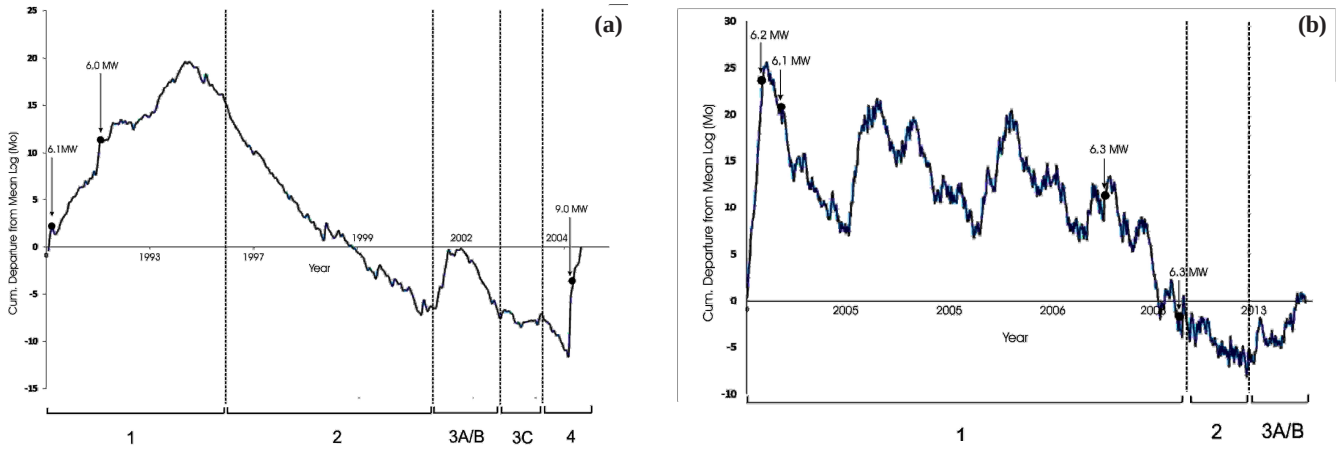

Fig.6. Hurst plot of years against cumulative difference from mean Log cumulative moment release data of earthquakes of Block C (Andaman – Sumatra subduction zone) **(a)** for the first earthquake cycle (1990-2004), ended with 2004 Sumatra earthquake (Mw 9.0). **(b)** for the second incomplete earthquake cycle (2005-2016). The phases are marked - elastic stress build-up (1), strain hardening (2), strain softening (3), dynamic failure (4) to generate earthquake event. Phase 3 is subdivided into 3A - crack coalescence, 3B - fluid diffusion phase and 3C- acceleration of fracture.

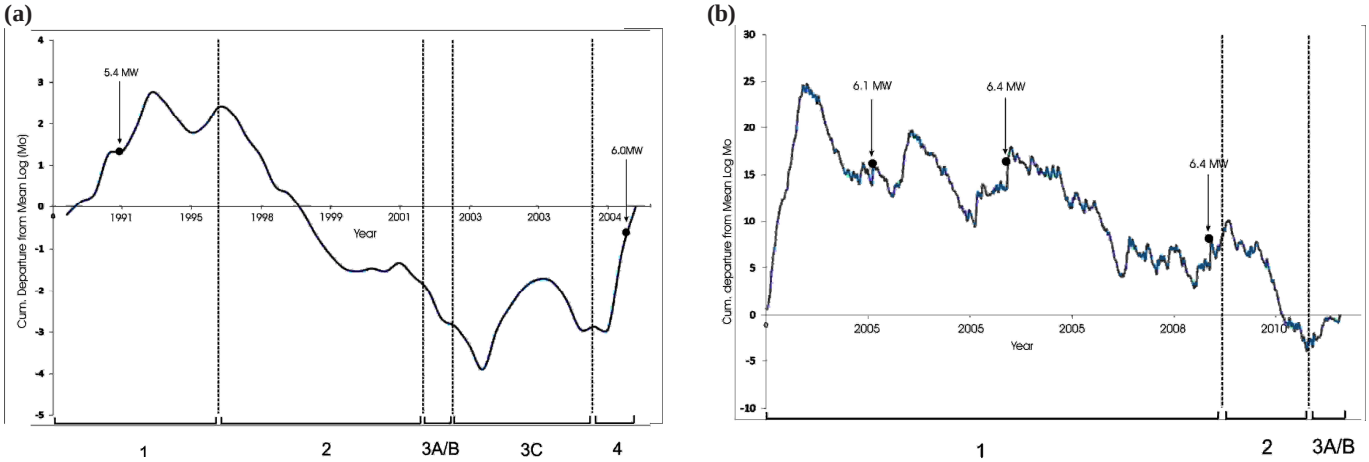

Fig.7. Hurst plot of years against cumulative difference from mean Log cumulative moment release data of earthquakes of Block D (Andaman – Sumatra subduction zone) (a) for the first earthquake cycle (1990-2004), ended with 2004 Sumatra earthquake (Mw 9.0). (b) for the second incomplete earthquake cycle (2005-2016). The phases are marked - elastic stress build-up (1), strain hardening (2), strain softening (3), dynamic failure (4) to generate earthquake event. Phase 3 is subdivided into 3A - crack coalescence, 3B - fluid diffusion phase and 3C- acceleration of fracture.

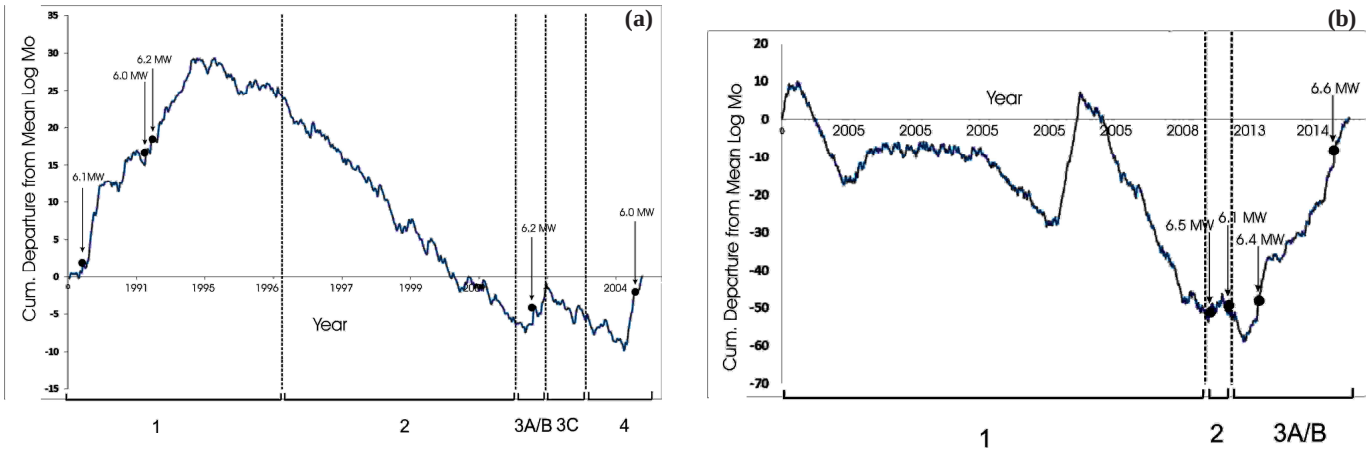

Fig.8. Hurst plot of years against cumulative difference from mean Log cumulative moment release data of earthquakes of Block E (Andaman – Sumatra subduction zone) **(a)** for the first earthquake cycle (1990-2004), ended with 2004 Sumatra earthquake (Mw 9.0). **(b)** for the second incomplete earthquake cycle (2005-2016). The phases are marked - elastic stress build-up (1), strain hardening (2), strain softening (3), dynamic failure (4) to generate earthquake event. Phase 3 is subdivided into 3A - crack coalescence, 3B - fluid diffusion phase and 3C- acceleration of fracture.

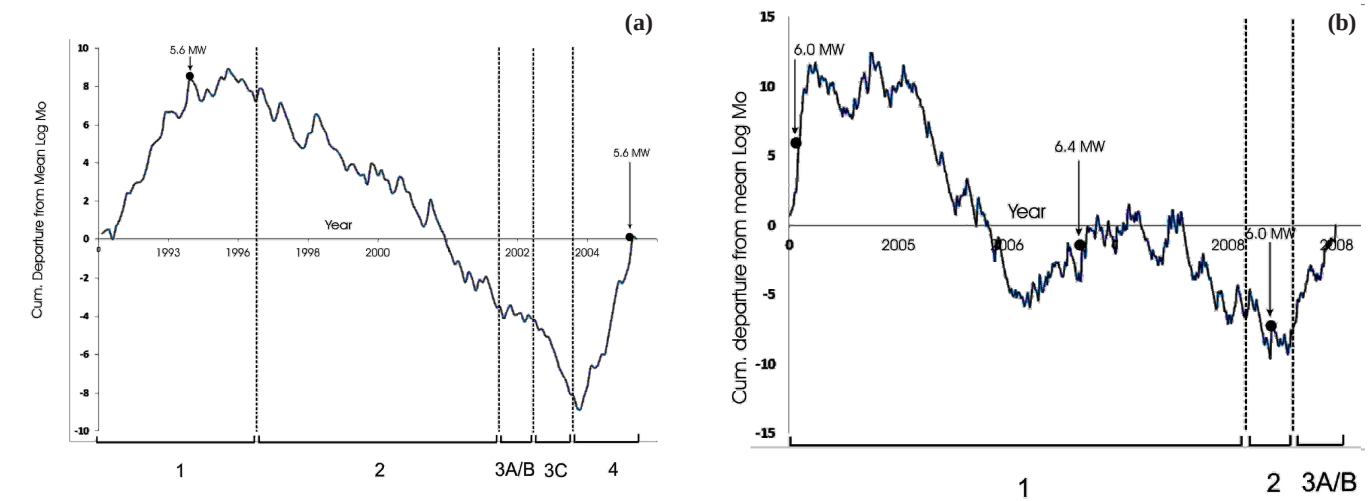

Fig.9. Hurst plot of years against cumulative difference from mean Log cumulative moment release data of earthquakes of Block F (Andaman – Sumatra subduction zone) **(a)** for the first earthquake cycle (1990-2004), ended with 2004 Sumatra earthquake (Mw 9.0). **(b)** for the second incomplete earthquake cycle (2005-2016). The phases are marked - elastic stress build-up (1), strain hardening (2), strain softening (3), dynamic failure (4) to generate earthquake event. Phase 3 is subdivided into 3A - crack coalescence, 3B - fluid diffusion phase and 3C- acceleration of fracture.

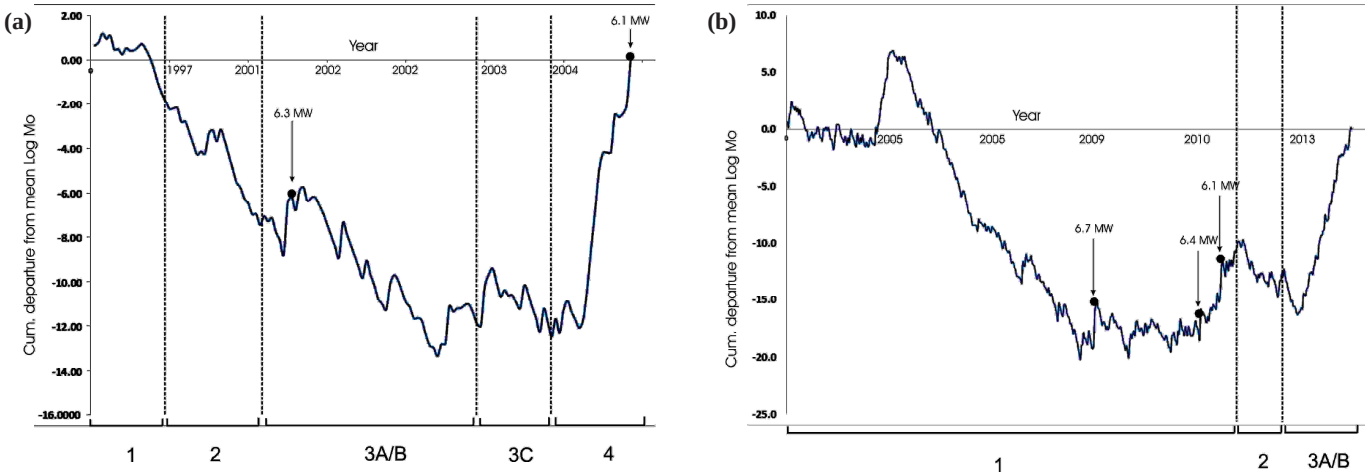

Fig.10. Hurst plot of years against cumulative difference from mean Log cumulative moment release data of earthquakes of Block G (Andaman – Sumatra subduction zone) **(a)** for the first earthquake cycle (1990-2004), ended with 2004 Sumatra earthquake (Mw 9.0). **(b)** for the second incomplete earthquake cycle (2005-2016). The phases are marked - elastic stress build-up (1), strain hardening (2), strain softening (3), dynamic failure (4) to generate earthquake event. Phase 3 is subdivided into 3A - crack coalescence, 3B - fluid diffusion phase and 3C- acceleration of fracture.

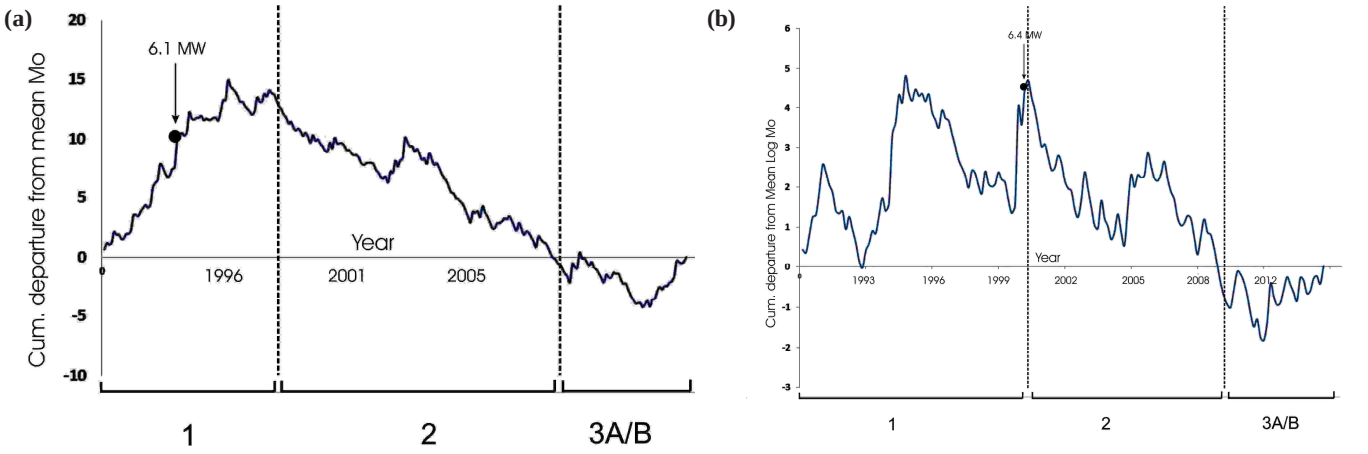

Fig.11. Hurst plot of years against cumulative difference from mean Log cumulative moment release data of earthquakes of **(a)** Block I and **(b)** Block M (Burma subduction zone) for the incomplete earthquake cycle (1990-2016). The phases are marked - elastic stress build-up (1), strain hardening (2), strain softening (3). Phase 3 is subdivided into 3A - crack coalescence, and 3B - fluid diffusion phase.

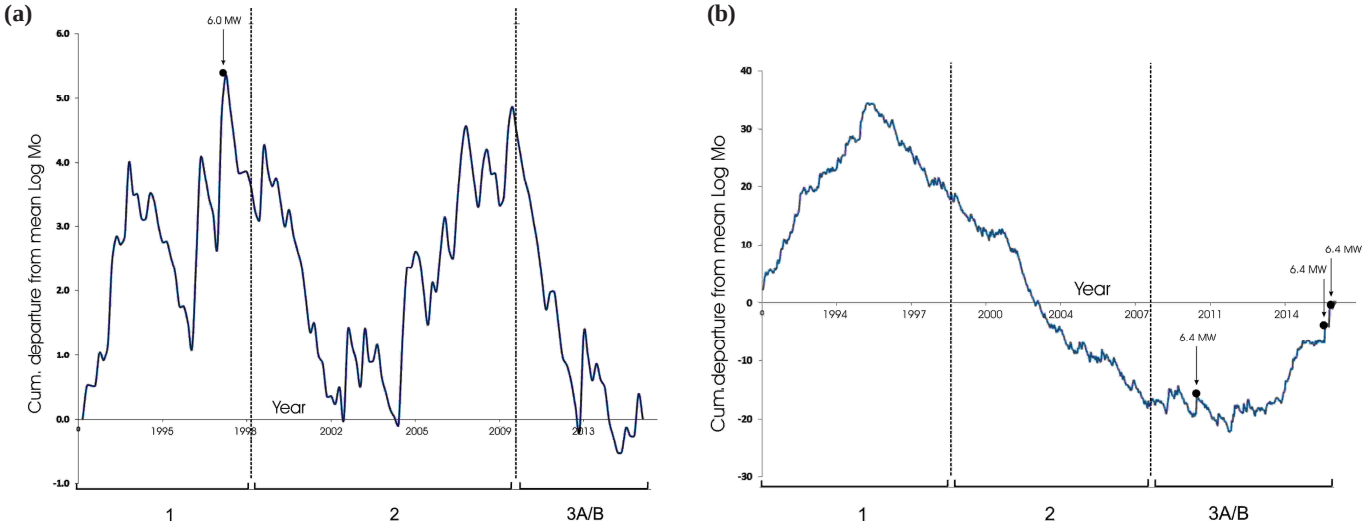

Fig.12. Hurst plot of years against cumulative difference from mean Log cumulative moment release data of earthquakes of **(a)** Block K and **(b)** Block L (Burma subduction zone) for the incomplete earthquake cycle (1990-2016). The phases are marked - elastic stress build-up (1), strain hardening (2), strain softening (3). Phase 3 is subdivided into 3A - crack coalescence, and 3B - fluid diffusion phase.

linear methods. They suggested that earthquake dynamics in this region are unstable but self-organized. Comparison of return maps of the data with random, stochastic, and chaotic time records shows quasi-deterministic behaviour (Tiwari and Krishnaveni, 2015) and hence the occurrence of earthquake may be predictable. This proposition is reviewed in the next sections.

Relationship between Seismic Cycles, Hurst Plot Patterns, and further Trend Analysis

Among the thirteen blocks (A to M) defined in the area based on their contrasting geo-tectonic characters, B to G (except block E) falls in the Benioff zone of Andaman – Sumatra sector, which has shown evidences of two consequent seismic cycles, one complete and another incomplete, within the period from 1990 to 2016 from the annual b-value plot (Fig.3). The Hurst plot for these blocks is analysed separately for two different seismic cycles, one started in 1990 and ended on 2004 while the other one started in 2005 and still being continued. Block I, L, M belongs to the subduction zone of Burma and shows evidence of one incomplete seismic cycle within 1990-2016 (Fig.4).

The Hurst plots (Figs. 5 - 12) for seismic cycle of each block are further segmented into different dynamic phases as per 'elastic failure model' of Main et al. (1989). The characteristic similarities of the Hurst pattern for the same dynamic phase of a seismic cycle across different blocks is observed. Such as, the phase of strain hardening (2) is always indicated by a short or prolonged negative slope. This phase ends with a sudden break in slope to form crack coalescence and fluid diffusion (3A&B) phase in the so far continuous negative slope of the Hurst plot. A subtle change in the slope of Hurst patterns is again present at the initiation of the phase of fracture acceleration (3C).

Having this characteristic relationship between Hurst plot and seismic cycles, the occurrence of major earthquakes are correlated. In all the blocks, major earthquake events occur only during three particular phases. All blocks have generated major and mostly the strongest earthquake during the phase of dynamic failure (4). In addition, few blocks (block B and E, Figs. 5a & 8a) have spawned larger earthquakes during the phase of crack coalescence and fluid diffusion (3A&B) phase also. Interestingly, the blocks where already a major earthquake occur during the phase 3A&B, do not give an earthquake of similar magnitude in its dynamic fracturing phase (4) possibly due to the loss of most of its accumulated strain during the last event. Incidentally, most of the blocks have consistently shown

occurrence of large earthquakes during the phase of elastic deformation, probably due to continued release of energy from previous cycle. However, none of the blocks has shown evidences of any major earthquake in the phase of strain hardening (2) or in the phase of acceleration of fracture (3C).

From the study of the seismic cycle and the Hurst pattern, it is concluded that every single block behaves similarly across the seismic cycles. The blocks that have given major earthquake during the phase of crack coalescence and fluid diffusion (3A&B) and have weaker dynamic failure earthquake (block B & E, Figs. 5a & 8a) in the first seismic cycle (1990-2004), behave similarly in the next seismic cycle (2005-2016) too (Figs. 5b & 8b). In the second cycle (2005-2016) where most of them has already given a crack coalescence & fluid diffusion phase (3A&B) earthquake, the dynamic failure (4) earthquake will probably not be as strong.

Similarly, the blocks (blocks C, D, F, Figs. 6a, 7a, 9a) that did not have any earthquake during crack coalescence and fluid diffusion phase (3A&3B) and the strongest earthquake of the cycle occurred during the dynamic failure phase (4) in first cycle (1990-2004), will not produce any large earthquake during the phase 3A&3B of the second seismic cycle (1990-2016) (Figs. 6b, 7b, 9b). It is possible that in these blocks the occurrence of strongest earthquake is still stored for the dynamic failure phase (4) of the second seismic cycle.

The block I, L and M belong to the subduction zone of Burma have shown evidence of a single incomplete seismic cycle from the annual b-value plot. Even this seismic cycle is an incomplete one as we can only confirm with confidence that end phase belongs to crack coalescence & fluid diffusion (3A&B). Within the Burma subduction zone, blocks I and L has already given large earthquakes (Mw 6.7 on 03.01.2016, Mw 6.9 on 13.04.2016 and Mw 6.8 on 24.08.2016) (Figs. 11a & 12b) that are inferred to be as crack coalescence and fluid diffusion phase (3A&B) earthquakes.

Identification of Most Vulnerable Blocks for Predicting Future Events

From the above discussions, few blocks with the possibility to generate impending large earthquake in the region can be identified. As already discussed, the blocks within the Benioff zone of Andaman – Sumatra sector acts similarly in both the seismic cycles. However, Block-G, though it has given a major earthquake during the crack coalescence and fluid diffusion phase (3A&3B) of the first seismic cycle (Fig.10a), it has not given any major earthquake to date in the 3A&3B phase of the second seismic cycle (2005-2016) (Fig. 10b). Therefore, we can consider Block-G as one of the most vulnerable blocks of the area.

Two blocks (I and L) among the Burma subduction zone blocks (blocks I, L, M) have already given major crack coalescence and fluid diffusion phase (3A&3B) earthquakes during the only seismic cycle identified in the region (Fig.12b). Although Block-M also belongs to this zone and has the same seismic cycle, it is yet to give a major earthquake for the phase (Figure 11b). Therefore, to our opinion Block-M can form another vulnerable zone for next major earthquake to occur.

Although Block-K was not considered within any of the two zones selected for determination of seismic cycles, it is surrounded by seismic blocks (G, I, L) that have already given or about to give crack coalescence and fluid diffusion phase (3A&B) earthquakes. However, Block-K has not yet given any major earthquake since long (Fig.12a). Therefore, there is a possibility that it may behave similarly as per the surrounding blocks to give a large earthquake in near future.

CONCLUSION

From the annual b-value analysis of Andaman – Sumatra subduction zone, we confirm presence of two consequent seismic cycles during the period of 1990-2016, where one started in 1990 and ended on 2004 and the other one started in 2005 and still having the phase of crack coalescence and fluid diffusion (3A&B). The subduction zone of Burma shows evidence of one incomplete seismic cycle within 1990-2016 that is continuing presently with crack coalescence and fluid diffusion (3A&B) phase.

References

Amorese, D., Grasso, J-R. and Rydelek, P.A. (2010) On varying b-values with depth: results from computer-intensive tests for Southern California. Geophys. Jour. Internat., v.180, pp.347–360.

Aki, K. (1965) Maximum likelihood estimate of *b* in the formula log N = a – bM and its confidence limits. Bull. Earthquake Res. Inst., Tokyo Univ., v.43, pp.237-239.

Chen, C., and Hiscott, R.N. (1999) Statistical analysis of turbidite cycles in submarine fan successions: Tests for short term persistence. Jour. Sediment. Res., v.69, pp.486-504.

Chan, L.S. and Chandler, A.M. (2001) Spatial bias in b-value of the frequency magnitude relation for the Hong Kong region. Jour. Asian Earth Sci., v.20, pp.73–81.

Curray, J.R. (2005) Tectonics and history of the Andaman Sea region. Jour. Asian Earth Sci., v.25, pp.187-232.

Dasgupta, S., Pande, P., Ganguly, D., Iqbal, Z., Sanyal, K., Venkatraman, N.V., Dasgupta, S., Sural, B., Harendranath, L., Mazumdar, S., Sanyal, S., Roy, A., Das, L.K., Misra, P.S., and Gupta, H. (2000) Seismotectonic Atlas of India and Its Environs. Geol. Surv. India Spec. Publ., Kolkata, India, 87p.

Dasgupta, S. and Mukhopadhyay, M. (1993) Seismicity and plate deformation below the Andaman Arc, Northeast Indian Ocean. Tectonophysics, v.225, pp.529–542.

Dasgupta, S., Mukhopadhyay, M., Bhattacharya, A., and Jana, T.K. (2003) The geometry of the Burmese–Andaman sub- ducting lithosphere. Jour. Seismol., v.7, pp.155–174.

Dasgupta, S., Mukhopadhyay, B. and Acharyya, A. (2007a) Seismotectonics of the Andaman- Nicobar Region: Constraints from Aftershocks within 24 Hours of the Great 26 December 2004 Earthquake
, In: Sumatra _ Andaman earthquake and Tsunami 26 December 2004 (Ed. Sujit Dasgupta), Geol. Surv. India, Spec. Publ., v.89, pp.95-104.

Dasgupta, S., Mukhopadhyay, B. and Bhattacharya, A. (2007b) Seismicity pattern in north Sumatra-Great Nicobar region: In search of precursor for the 26 December 2004 earthquake. Jour. Earth System Sci., v.116(3), pp.215-223.

Dasgupta, S., Mukhopadhyay, B. and Acharyya, A. (2005) Aftershock propagation characteristics during the first three hours following the 26 December 2004 Sumatra-Andaman Earthquake, Gondwana Res., v.8, pp.585-588.

Hanks, H.C. and Kanamori,, H. (1979) A moment magnitude scale. Jour. Geophys. Res., v.84, pp.2348-2350. DOI: 10.1029/JB084iB05p02348.

Hurst, H.E. (1951) Long term storage capacity of reservoirs. T. Amer. Soc. Civil Engg., v.116, pp.770–808.

Hurst, H.E. (1956) Methods of using long-term storage in reservoirs. Proc. Inst. Civil Engg., Part 1, 5, pp.519–590.

Kafka, A.L., and Walcott, J.R. (1998) How well does the spatial distribution of smaller earthquakes forecast the locations of larger earthquakes in the Northeastern United States? Seismol. Res. Lett., v.69, pp.428–440.

Klotz, J., Khazaradze, G., Angermann, D., Reigber, C., Perdomo, R. and Cifuentes, O. (2001) Earthquake cycle dominates contemporary crustal deformation in Central and Southern Andes. Earth Planet. Sci. Lett., v.193, pp.437-446.

Kulhanek, O. (2005) Seminar on b-value. Department of Geophysics, Charles University, December 10–19, 2005, Prague.

Mandelbrot, B., and Hudson, R.L. (2004) The (Mis)Behavior of Markets, A Fractal View of Risk, Ruin and Reward, Basic Books -Business & Economics, Profile Book, London, 329p.

Mansukhani, S. (2012) The Hurst Exponent: Predictability of Time Series, Analytics Magazine, Issue July/August 2012, http://analytics-magazine.org/the-hurst-exponent-predictability-of-time-series/

Main, I.G., Meredith, P. and Jones, C. (1989) A reinterpretation of the precursory seismic b-value anomaly from fracture mechanics. Geophys. Jour. Internat., v.96, pp.131–138.

Mcguire, R.K. (2004) Seismic Hazard and Risk Analysis, EERI Monograph 10, Earthquake Engineering Research Institute, Oakland, California, USA.

Mukhopadhyay, B., Chakraborty, P.P. and Paul, S. (2003) Facies clustering in turbidite successions: Case study from Andaman Flysch Group, Andaman Islands, India. Gondwana Res., v.6, pp.918–925. DOI: 10.1016/S1342-937X(05) 71036-4.

Mukhopadhyay, B., Acharyya, A., and Dasgupta, S. (2009a) Statistical Analysis on Yearly Seismic Moment Release Data to Demarcate the Source Zone for an Impending Earthquake in the Himalaya. Acta Geophysica, v.57(2), pp.387–399. DOI: 10.2478/s11600-008-0068-0

Mukhopadhyay, B., Acharyya, A., Bhattacharya, A., Dasgupta, S., and Sengupta, S.R. (2009b) Revisiting the Andaman subduction lithosphere following the 26 December 2004 Sumatra earthquake. Indian Jour. Geosci., v.63(1), pp.1–10.

Mukhopadhyay, B. and Sengupta, D. (2018) Seismic moment release data in earthquake catalogue: application of Hurst Statistics in delineating temporal clustering and seismic vulnerability. Jour. Geol. Soc. India, v.91, pp.15-24.

Nuannin, P. (2006) The potential of b-value variations as earthquake precursors for small and large events, Doctoral dissertation, Acta Universitatis Upsaliensis.

Nuannin, P., Kulhánek, O. and Persson, L. (2012) Variations of b-values preceding large earthquakes in the Andaman-Sumatra subduction zone. Jour.Asian Earth Sci., v.61, pp.237-242.

Sandri, L. and Marzocchi, W. (2007) A technical note on the bias in the estimation of the b-value and its uncertainty through the least squares technique. Annals of Geophysics, v.50, pp.329–339

Scordilis, E.M. (2006) Empirical global relations converting MS and mb to moment magnitude. Jour. Seismol., v.10, pp.225–236.

Shi, Y., and Bolt, B.A. (1982) The standard error of the magnitude-frequency b-value. Bull. Seismol. Soc. Amer., v.721, pp.1677–1687.

Srivastava, K., Rani, S. and Srinagesh, D. (2015) A review of b-value imaging and fractal dimension studies in the Andaman Sumatra subduction. Natural Hazards, v.77(1), pp.97-107.

Tormann, T., Enescu, B., Woessner, J. and Wiemer, S. (2015) Randomness of megathrust earthquakes implied by rapid stress recovery after the Japan earthquake. Nature Geoscience, v.8(2), pp.152-158.

Tiwari, R.K. and Krishnaveni, P. (2015) Evidence of self-organization in Sumatra earthquakes: recurrence time and its geodynamical implications. Natural Hazards, v.77, Supplement 1, pp.51–63.

Uyeda, S. and Kanamori, H. (1979) Back-arc opening and the mode of subduction. Jour.f Geophys. Res., v.84, pp.1049–1061.

Wallis, J.R. and Matalas, N.C. (1970) Small sample properties of H and K estimators of Hurst coefficient h. Water Resour. Res., v.6, pp.1583-1594. DOI: 10.1029/ WR006i006p01583.

Wallis, J.R. and Matalas, N.C. (1971) Correlogram analysis revisited. Water Resour. Res., v.7, pp.1448–1459. DOI: 10.1029/WR007i006p01448.

Wang, K.L., Hu, Y. and He, J.H. (2012) Deformation cycles of subduction earthquakes in a viscoelastic Earth. Nature, v.484, pp.327- 332.

Wiemer, S. and Wyss, M. (2000) Minimum magnitude of completeness in earthquake catalogs: example from Alaska, the western United States, and Japan. Bull. Seismol. Soc. Amer., v.90(4), pp.859–869.

(Received: 28 July 2017; Revised form accepted: 19 March 2018)